Observation of Quantum Capacitance in the Cooper-Pair Transistor

T. Duty,* G. Johansson, K. Bladh, D. Gunnarsson, C. Wilson, and P. Delsing
Microtechnology and Nanoscience, MC2, Chalmers University of Technology, S-412 96 Göteborg, Sweden
(Received 30 March 2005; published 11 November 2005)

We have fabricated a Cooper-pair transistor (CPT) with parameters such that for appropriate voltage biases, it behaves essentially like a single Cooper-pair box (SCB). The effective capacitance of a SCB can be defined as the derivative of the induced charge with respect to gate voltage and has two parts, the geometric capacitance, C_{geom}, and the quantum capacitance C_Q. The latter is due to the level anticrossing caused by the Josephson coupling and is dual to the Josephson inductance. It depends parametrically on the gate voltage and its magnitude may be substantially larger than C_{geom}. We have detected C_Q in our CPT, by measuring the in phase and quadrature rf signal reflected from a resonant circuit in which the CPT is embedded. C_Q can be used as the basis of a charge qubit readout by placing a Cooper-pair box in such a resonant circuit.

DOI: 10.1103/PhysRevLett.95.206807 PACS numbers: 74.50.+r, 85.25.Cp, 03.67.Lx, 03.65.−w

The quantum-mechanical properties of the single Cooper-pair box (SCB) [1,2]—an artificial two-level system—have been investigated thoroughly during the last few years due to the potential for SCB's to serve as quantum bits (qubits) [3–7]. An important property of SCB qubits is the existence of an optimal point, where the first derivative of the energy bands with respect to gate voltage vanishes, and the system is insensitive to low-frequency charge fluctuations [5,7]. Dephasing times are maximum at this point, making it the natural operation point for single-qubit quantum rotations. Since the eigenstates at the optimal point are orthogonal to charge eigenstates, however, one must move away from the optimal point for readout schemes based upon charge measurement.

A recent experiment used the polarizability of an SCB coupled to a microwave resonator to perform cavity-QED measurements [8]. Such a circuit can also perform a quantum nondemolition measurement of the qubit state at the optimal point. In this Letter, we study a type of polarizability that can be described as an effective capacitance and is related to the second derivative, or curvature, of the energy bands with respect to gate voltage. This quantum capacitance was first discussed in the context of small Josephson junctions [9–11] and is dual to the Josephson inductance. Recently, a controllable coupling scheme based upon this parametric capacitance [12] has been proposed, as well as a superconducting phase detector [13].

Both the single-electron transistor (SET) [14,15] and its superconducting version, also known as the Cooper-pair transistor (CPT) [16], are closely related to the SCB. These devices are the basis of very sensitive electrometers that are used to readout charge qubits [6,7,17]. Previous work concentrated on the dissipative response and backaction of SET's and CPT's when used as electrometers [18–21]. Here, we show that an appropriately designed CPT can also exhibit a reactive response due to quantum capacitance. This capacitance can be measured using a radio-frequency resonant circuit.

To see how quantum capacitance arises, we first consider the single Cooper-pair box as depicted in Fig. 1(a). The box has a Josephson energy E_J, charging energy $E_C = e^2/2C_\Sigma$, and total capacitance $C_\Sigma = C_J + C_g$. The effective capacitance can be defined as the first derivative of the injected charge with respect to voltage, $C_{\mathrm{eff}} = \partial\langle Q_g\rangle/\partial V_g$, where the brackets denote a quantum expectation value. From electrostatics, one has $Q_g = C_g(V_g - V_{\mathrm{island}})$, and $V_{\mathrm{island}} = (C_g V_g - 2en)/C_\Sigma$, so that

$$\langle Q_g\rangle = \frac{C_g C_J}{C_\Sigma} V_g + 2e\langle n\rangle \frac{C_g}{C_\Sigma}, \tag{1}$$

where n is the number of Cooper pairs that have tunneled onto the island. For each energy band k of the SCB, $\langle n\rangle$ depends on the normalized gate charge $n_g = C_g V_g/e$. One finds that

$$C^k_{\mathrm{eff}} = \frac{C_g C_J}{C_\Sigma} - \frac{C_g^2}{e^2}\frac{\partial^2 E_k}{\partial n_g^2} = C_{\mathrm{geom}} + C^k_Q \tag{2}$$

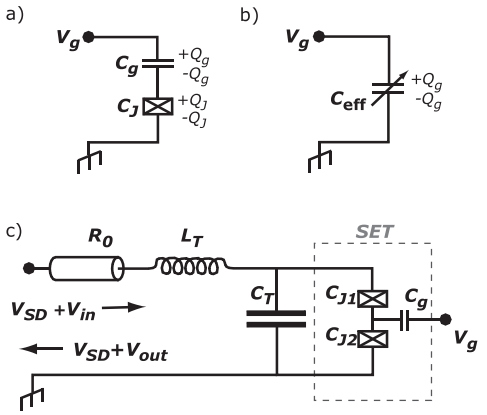

FIG. 1. (a) The Cooper-pair box and (b) its equivalent as a parametric capacitor. (c) Schematic of the rf-SET. A monochromatic radio-frequency signal V_{in}, added to a dc voltage bias V_{SD}, is reflected from a tank circuit containing the SET.

where $C_{\rm geom}$ is the *geometric* capacitance of two capacitors in series, and $C_Q^k \equiv -(C_g^2/e^2)(\partial^2 E_k/\partial n_g^2)$ is the *quantum* capacitance. In the two-level approximation, which is valid for $\epsilon \equiv E_J/4E_C \ll 1$, the ground and first excited state energies are given by $E_\pm = \pm 2E_C\sqrt{(1-n_g)^2+\epsilon^2}$. These produce the quantum capacitances

$$C_Q^\pm = \mp \frac{C_g^2}{C_\Sigma}\epsilon^2[(1-n_g)^2+\epsilon^2]^{-3/2}. \quad (3)$$

The magnitude of C_Q is maximum at the charge degeneracy,

$$C_Q^\pm(n_g=1) = \mp \frac{2e^2}{E_J}\frac{C_g^2}{C_\Sigma^2}. \quad (4)$$

We note that although C_Q grows with decreasing E_J, the region of n_g where it is observable becomes vanishingly small. The value of e^2/h is approximately 40 fF GHz, so a charge qubit (SCB) with $E_J/h = 10$ GHz and $C_g = C_J$ would have a quantum capacitance at the charge degeneracy of 2 fF, which is higher than the typical junction capacitance ($C_J \sim 1$ fF) of a charge qubit.

For finite temperatures, a Boltzmann-weighted average of the injected charge must be considered, giving the effective capacitance

$$C_{\rm eff} = \frac{C_g C_J}{C_\Sigma} - \frac{C_g^2}{e^2}\frac{\partial}{\partial n_g}\left\langle \frac{\partial E_k}{\partial n_g}\right\rangle_{\rm T}. \quad (5)$$

We now turn to the CPT, which consists of a metallic island connected to two leads by small capacitance tunnel junctions [see Fig. 1(c)]. An external gate controls the potential of the island through the gate-induced charge on the island, $n_g = C_g V_g/e$. If $E_J/4E_C \ll 1$, an appreciable direct quasiparticle (QP) current occurs only when $eV_{\rm SD} > 4\Delta$. For smaller bias voltages, a gate-dependent subgap current is possible due to sequences of Cooper-pair tunneling combined with QP tunneling. These processes are known as Josephson-quasiparticle (JQP) cycles [22–26]. Recent research has focused upon describing the noise and backaction effects of such JQP processes—when they carry a substantial current [20,21]. For a JQP process to carry a substantial current, however, the QP tunneling rates must be relatively fast. We have constructed a CPT where these rates are very slow in a certain region of voltage bias $V_{\rm SD}$. This region of $V_{\rm SD}$ is centered at $eV_{\rm SD} = 2E_C$, at the intersections of lines in the $V_{\rm SD}$-n_g plane where Cooper-pair tunneling across one junction is resonant (see Fig. 2). This intersection is known as the double JQP (DJQP) point.

Charge transport in this region of $V_{\rm SD}$ consists of QP tunneling events that move the system between two Josephson-coupled charge manifolds [21]. E.g., for $n_g \in [0,1]$, the QP transitions link the $0 \leftrightarrow 2$ and $-1 \leftrightarrow 1$ manifolds [see Fig. 2(b)]. The QP tunneling rate $\Gamma_{\rm QP}$ depends on dE, the energy gain of the tunnel event. It is large only when dE exceeds 2Δ [27]. At the DJQP point,

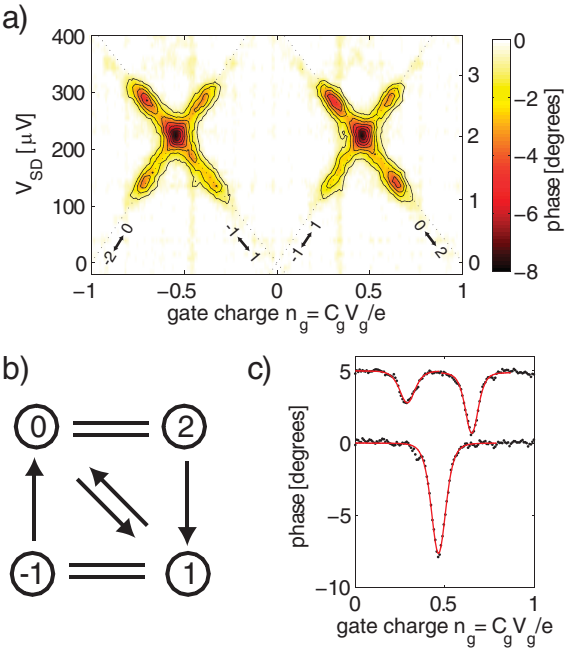

FIG. 2 (color online). (a) Phase shifts around $eV_{\rm SD} = 2E_C$. Cooper-pair tunneling between the indicated charge states is degenerate across junction 1 (2) along the dotted lines with positive (negative) slope. The right y axis is in units of reduced bias, $v = eV_{\rm SD}/E_C$. (b) Diagram of the charge states involved in the JQP processes for gate charge $0 < n_g < 1$. The solid lines with arrows represent tunneling of quasiparticles and the double lines Cooper pairs. The upper right triangle represents transitions occurring along the negative-slope dotted line in (a), and the bottom left triangle those along the positive-slope line. (c) Phase shifts vs gate charge for $V_{\rm SD} = 222$ μV (lower points) and $V_{\rm SD} = 145$ μV (upper points, offset 5 degrees for clarity). The solid lines are the theoretical expectations using Eq. (5) and the two-level approximation, the values of E_J found from spectroscopy, and $T = 130$ mK.

$dE = 3E_C$, and hence QP tunneling is suppressed if $E_C < 2\Delta/3$ [22,26], which is the case for the CPT considered here, $E_C \simeq \Delta/2$. The measured dc current at the DJQP point is less than $\sim$1 pA, which indicates a QP tunneling rate $\sim$4 MHz. Because the QP rates are very slow compared to the Cooper-pair tunneling rate ($\sim$ 3 GHz) and the intramanifold relaxation rate ($\sim$ 1 GHz, see below), this CPT behaves essentially like a SCB, where Cooper pairs tunnel coherently across one junction while the other junction acts as a gate capacitance. This picture is interrupted at long time scales by incoherent QP tunnel events.

This description breaks down in a small region around zero bias, where the eigenstates are those of definite phase across the CPT. For $eV_{\rm SD} \ll E_C$, C_Q becomes sensitive to low-frequency fluctuations of the phase. Consequently, we do not observe C_Q around zero bias, which could also be due to poisoning by nonequilibrium QP's.

We fabricated a CPT using e-beam lithography and standard double-angle shadow evaporation of aluminum onto an oxidized silicon substrate. The sample was placed

at the mixing chamber of a dilution refrigerator with a base temperature of ≈ 20 mK. All dc control lines were filtered by a combination of low-pass and stainless steel powder filters. The measured normal resistance of the SET was $R_n = 120\ \mathrm{k}\Omega$ which implies a Josephson energy $E_J = 12\ \mu\mathrm{eV}$ ($E_J/h = 2.9$ GHz) per junction using the Ambegaokar-Baratoff relation [28]. $E_C = 111\ \mu\mathrm{eV}$, and $\Delta = 215\ \mu\mathrm{eV}$, were determined from the DC-IV curves .

Our CPT was configured as a radio-frequency SET (rf-SET) [29], which is based upon reflection of a monocromatic radio-frequency signal from a tank (LC) circuit containing the SET [see Fig. 1(c)]. The tank circuit described here had a resonant frequency of 342 MHz using a inductance $L_T = 490$ nH, which implies a tank circuit capacitance $C_T = 440$ fF coming from the stray capacitance of the bonding pad connecting the inductor to the chip. The CPT has a reactive response due to its effective capacitance. Like that of the SCB, it is related to second derivatives of the energy bands. In this case, the derivatives are with respect to the source-drain voltage V_{SD}, and one must tune both V_{SD} and n_g to sit at a Cooper-pair charge degeneracy. One finds a form similar to Eq. (3) but with $C_\Sigma = C_{J1} + C_{J2} + C_g$. For a symmetric transistor ($C_{J1} = C_{J2}$) and $C_g \ll C_{J1}$ the expression is identical to Eq. (3), but with $1 - n_g$ replaced by $1 - n_g - \upsilon/4$, where $\upsilon = eV_{\mathrm{SD}}/E_C$.

The reflection coefficient for the circuit of Fig. 1(c) is given by $\alpha = V_{\mathrm{out}}/V_{\mathrm{in}} = (Z - Z_0)/(Z + Z_0)$, with

$$Z = i\omega L_T + (i\omega C + R_{\mathrm{SET}}^{-1})^{-1}, \tag{6}$$

where $C = C_T + C_{\mathrm{eff}}$ is the total capacitance, and $Z_0 \simeq 50\ \Omega$. C_{eff} is the effective capacitance of the CPT, which depends on both V_{SD} and n_g. If $R_{\mathrm{SET}} \gg L/Z_0C \simeq 23\ \mathrm{k}\Omega$ for our circuit, the phase of α near resonance is only affected by changes in C. It will be convenient to fix the total capacitance (and hence phase) relative to some particular value of V_{SD} and n_g, where $C_Q = 0$. We write $C = C_0 + C_Q$. We define the detuning parameter $\delta = 1 - \omega/\omega_0$, with $\omega_0 = 1/\sqrt{L_T C_0}$ and $\omega = 1/\sqrt{L_T C}$. For $2Q\delta \ll 1$, one finds $\alpha = -1 + i4Q\delta$, where the quality factor $Q = \sqrt{L_T/C}/Z_0 = 21$ for our circuit, and $\delta = C_Q/2C_0$. Then the phase of the reflected signal is

$$\theta = \tan^{-1}(-2QC_Q/C_0). \tag{7}$$

For our measurements, an rf excitation of -119 dBm ($V_{\mathrm{in}} \simeq 0.2\ \mu\mathrm{V}$) was reflected from the tank circuit. The in-phase and quadrature signals from the mixer were low-pass filtered using a cutoff frequency of 10 kHz. For each value of V_{SD}, V_g was ramped at 237 Hz and 1024 repetitions of the signal were acquired and averaged taking a few seconds. Below $eV_{\mathrm{SD}} = 4E_C$ only a small modulation of the magnitude of the reflected rf excitation was observed, corresponding to $R_{\mathrm{SET}} > 1\ \mathrm{M}\Omega$. This value of R_{SET} is much too large to produce the phase shifts observed at these biases as described above. In Fig. 2(a) we show the phase shift of the reflected signal as a function of V_{SD} and n_g. The phase shifts fall along the Cooper-pair degeneracies and are concentrated in characteristic "X" patterns around the DJQP points with a maxima at the center. The X's are cut off for $eV_{\mathrm{SD}} < E_C$ and for $eV_{\mathrm{SD}} \gtrsim 3E_C$. This pattern can be understood by considering the QP tunneling rates involved in the JQP cycles and illustrated in Fig. 2(b). For gate charge $n_g \in [0, 1]$, the charge states 0 and 2 are degenerate along the negative-slope dotted line, $\upsilon = -4(n_g - 1)$, in the right half of Fig. 2(a). The charge states -1 and 1 are degenerate along the positive-slope line, $\upsilon = 4n_g$. The QP rates depend on dE. For a QP transition from charge state n to $n \pm 1$, $dE_{n\to n\pm1}/E_C = \mp 2(n - n_g) - 1 + \upsilon/2$. The relevant rates are those along the Cooper-pair degeneracies. Between $eV_{\mathrm{SD}} = E_C$ and $eV_{\mathrm{SD}} = 3E_C$, the QP transitions, e.g., $2 \to 1$ and $1 \to 0$, involve an energy gain $dE < 2\Delta$, and hence these rates are small [22,26]. Nevertheless, away from the DJQP point, the system spends some fraction of time in a nondegenerate charge state, which reduces the observed phase shift. One observes a maximum phase shift precisely at the DJQP, since both the $0 \leftrightarrow 2$ and $-1 \leftrightarrow 1$ manifolds are at their Cooper-pair charge degeneracies, despite the QP transitions that move the system slowly from one manifold to the other. For $eV_{\mathrm{SD}} < E_C$, the QP transition $1 \to 0$, along the $0 \leftrightarrow 2$ Cooper-pair degeneracy, involves an energy cost; therefore, this rate is thermally suppressed, and the system gets stuck in the nondegenerate state 1. For $eV_{\mathrm{SD}} \gtrsim 3E_C$, since $E_C \simeq \Delta/2$, the QP transition $2 \to 1$, along the $0 \leftrightarrow 2$ degeneracy, has an energy gain greater than 2Δ and becomes exponentially larger. Again, the system is trapped in the nondegenerate state 1. A similar argument applies to QP transition rates along the $-1 \leftrightarrow 1$ degeneracy.

In Fig. 2(c) we show the phase shift versus gate charge for $eV_{\mathrm{SD}} = 2E_C$, i.e., crossing the DJQP, and for $eV_{\mathrm{SD}} = 1.35E_C$. We can fit the measured phase shifts using the two-level approximation and Eq. (5), and get good agreement using the values of E_J found from the spectroscopic measurements discussed below, if we allow for a nonzero temperature. A second free parameter is an overall constant, which is reduced from the value $2Q$ in Eq. (7) due to imperfections of our microwave circuitry, e.g., a less than ideal directivity of the directional coupler used in our setup. This constant is further reduced away from the DJQP point due to the relative time spent in the nondegenerate manifold. The extracted temperature is $T = 130$ mK, which is higher than the bath temperature $T \simeq 20$ mK. This could be due to self-heating from the small ~ 1 pA current produced by the JQP cycles [30]. Another factor contributing to the elevated temperature could be noise from the cold amplifier, which can be reduced by using a cold microwave circulator.

We can make a more direct measurement of E_J for each junction by applying microwaves to the gate of the transistor. Resonant microwave radiation induces transitions to the excited state, which has a capacitance of the opposite

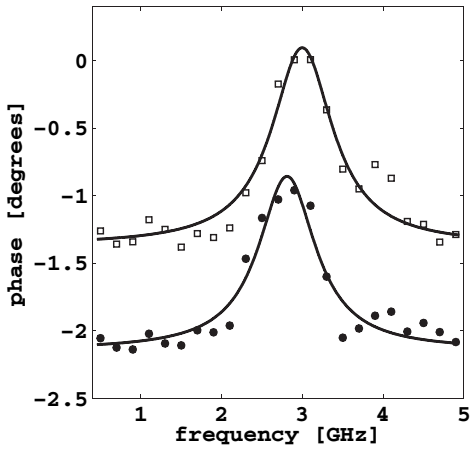

FIG. 3. Microwave spectroscopy for $V_{SD} = 170\ \mu$V and gate charge n_g tuned to the Cooper-pair resonance of junction 1 (upper data) and junction 2 (lower data). The lower data set has been offset -1 degrees for clarity. The solid lines are fits to a Lorentzian and produce frequencies 3.0 MHz for junction 1, and 2.8 MHz for junction 2, and a FWHM of 0.9 MHz for both.

sign. Figure 3 shows the effects of microwaves on the phase shift when the transistor is tuned in V_{SD} and n_g to be at the Cooper-pair degeneracy for the individual junctions. The data are fit to Lorentzians, and the resulting values $E_J/h = 3.0$ GHz for junction 1, and $E_J/h = 2.8$ GHz for junction 2 agree well with the estimate 2.9 GHz derived from the normal state resistance using the Ambegaokar-Baratoff relation. The full width at half maximum (FWHM) of both fits is 0.9 GHz. It is due to lifetime broadening and indicates a relaxation time $T_1 = 1.1$ ns, which is consistent with our previous measurements on charge qubits [7], given that this transistor is more strongly coupled to its environment.

A suitable device for studying the quantum capacitance in detail would consist of a SCB placed in a rf tank circuit. An electrometer based upon such a rf SCB device could go beyond the so-called shot noise limit, which is due to the source-drain current in the transistor [17,19]. Moreover, the rf SCB would form an integrated charge qubit and readout device. While this has been done using microwave resonators to reach the cavity-QED, strong-coupling limit [8], we suggest that it is not necessary to go to such an extreme quantum limit simply for qubit readout. Instead, one can use lower-frequency lumped circuits that utilize the quantum capacitance, i.e., the response of the SCB to classical electromagnetic fields. Using lower-frequency resonators may further shield the qubit from the high-frequency fluctuations of the electromagnetic environment.

In conclusion, we have observed the quantum contribution to the effective capacitance of a Cooper-pair transistor by measuring the gate-dependent phase shift of a resonant circuit in which the transistor is embedded. The measured phase shifts are in good agreement with a theory that takes into account a finite temperature and the combined tunneling of Cooper pairs and quasiparticles.

We would like to acknowledge helpful discussions with V. Shumeiko. The work was supported by the Swedish SSF and VR, by the Wallenberg foundation, and by the EU under the IST-SQUBIT-2 programme.

*Electronic address: tim@mc2.chalmers.se

[1] M. Büttiker, Phys. Rev. B **36**, 3548 (1987).
[2] V. Bouchiat *et al.*, Phys. Scr. **T76**, 165 (1998).
[3] Y. Nakamura, Y. A. Pashkin, and J. S. Tsai, Nature (London) **398**, 786 (1999).
[4] Y. Makhlin, G. Schön, and A. Shnirman, Rev. Mod. Phys. **73**, 357 (2001).
[5] D. Vion *et al.*, Science **296**, 886 (2002).
[6] K. W. Lehnert *et al.*, Phys. Rev. Lett. **90**, 027002 (2003).
[7] T. Duty *et al.*, Phys. Rev. B **69**, 140503(R) (2004).
[8] A. Wallraff *et al.*, Nature (London) **431**, 162 (2004).
[9] A. Widom *et al.*, J. Low Temp. Phys. **57**, 651 (1984).
[10] D. V. Averin, A. B. Zorin, and K. K. Likharev, Sov. Phys. JETP **61**, 407 (1985).
[11] K. K. Likharev and A. B. Zorin, J. Low Temp. Phys. **59**, 347 (1985).
[12] D. V. Averin and C. Bruder, Phys. Rev. Lett. **91**, 057003 (2003).
[13] L. Roschier, M. Sillanpää, and P. Hakonen, Phys. Rev. B **71**, 024530 (2005).
[14] T. A. Fulton and G. J. Dolan, Phys. Rev. Lett. **59**, 109 (1987).
[15] K. K. Likharev, IEEE Trans. Magn. **23**, 1142 (1987).
[16] A. B. Zorin, Phys. Rev. Lett. **76**, 4408 (1996).
[17] A. Aassime *et al.*, Appl. Phys. Lett. **79**, 4031 (2001).
[18] A. Aassime *et al.*, Phys. Rev. Lett. **86**, 3376 (2001).
[19] G. Johansson, A. Käck, and G. Wendin, Phys. Rev. Lett. **88**, 046802 (2002).
[20] M. S. Choi, F. Plastina, and R. Fazio, Phys. Rev. Lett. **87**, 116601 (2001).
[21] A. A. Clerk *et al.*, Phys. Rev. Lett. **89**, 176804 (2002).
[22] T. A. Fulton *et al.*, Phys. Rev. Lett. **63**, 1307 (1989).
[23] D. V. Averin and V. Ya. Aleshkin, JETP Lett. **50**, 367 (1989).
[24] A. Maassen van den Brink, G. Schön, and L. J. Geerligs, Phys. Rev. Lett. **67**, 3030 (1991).
[25] A. Maassen van den Brink *et al.*, Z. Phys. B **85**, 459 (1991).
[26] Y. Nakamura, C. D. Chen, and J. S. Tsai, Phys. Rev. B **53**, 8234 (1996).
[27] M. Tinkham, *Introduction to Superconductivity* (Dover, New York, 2004), 2nd ed., p. 77.
[28] V. Ambegaokar and A. Baratoff, Phys. Rev. Lett. **10**, 486 (1963).
[29] R. J. Schoelkopf *et al.*, Science **280**, 1238 (1998); **11**, 104(E) (1963).
[30] Calculations as described in Verbrugh *et al.*, J. Appl. Phys. **78**, 2830 (1995) for self-heating in single-electron devices, using the parameters of our sample, give $T \simeq 150$ mK.